Islamic Azad University

Journal of

Optoelectronical Nanostructures

Spring 2018 / Vol. 3, No. 2

Effect of Annealing on Physical Properties of Cu_2ZnSnS_4 (CZTS) Thin Films for Solar Cell Applications

Heydar Izadneshan[*,1], Ghahraman Solookinejad[1]

[1]Department of physics, Marvdasht Branch, Islamic Azad University, Marvdasht, Iran.

(Received 20 Mar. 2018; Revised 14 Apr 2018; Accepted 23 May 2018; Published 15 Jun. 2018)

Abstract: Cu2ZnSnS4 (CZTS) thin films were prepared by directly sputtering Cu (In,Ga)Se2 quaternary target consisting of (Cu: 25%, Zn: 12.5%, Sn; 12.5% and S: 50%). The composition and structure of CZTS layers have been investigated after annealing at 200 ^{0}C, 350 ^{0}C and 500 0C under vacuum. The results show that recrystallization of the CZTS thin film occurs and increasing the grain size with a preferred orientation in the (112) direction was obtained. The Raman spectra showed the existence of crystalline CZTS phase after annealing. Optical transmission spectra were recorded within the range 300-900 nm. The energy band gap (Eg) of the CZTS thin films was calculated before and after annealing from the transmittance spectra using Beer-Lambert's law. Results show that Eg is dependent on the annealing temperature. The optical band gap of CZTS also varied from 1.57 eV to 1.31 eV with increase in the annealing temperature from 200 ^{0}C min to 500 ^{0}C.

Keywords: CZTS, Magnetron Sputtering, Optical Properties, Solar Cells.

1. INTRODUCTION

Multinary compounds semiconductor, Cu_2ZnSnS_4 (CZTS) and $Cu_2ZnSn(S, Se)_4$ (CZTSSe) with kesterite crystal structure are promising materials for high efficiency thin film solar cell absorber layers because they have high absorption coefficient (104 cm^{-1}), low processing cost, not including rare metal, and suitable direct band gap (1.4 eV) for solar spectrum [1–3]. The CZTS semiconductor is potential candidate material for terawatt (TW) scale photovoltaic energy conversion: a fractional amount of the elemental constituents produced annually solar cells which can supply renewable energy on a scale comparable to is

* Corresponding author. E-mail: **izadneshan@yahoo.com**

sufficient to fabricate CZTS thin-film the world's electricity consumption [4-7]. Significant progress on this relatively new research area has been achieved in recent years [5-6]. Champion efficiency of CZTS thin film solar cell has reached 8.8 % and an efficiency of 6.21 % has been demonstrated for CZTS solar cells [7-9]. However, these efficiencies are still much lower than those of CIGS PV devices. Therefore new research based on improve efficiency and preparation cost of CZTS thin film solar cells [8,9]. So the purpose of this work is firstly to investigate the effect of preparation condition on structural and optical properties of CZTS thin films [10].

2. FABRICATION PROCEDURES

Quartz glass was used as a substrate after Molybdenum (Mo) back contact with 500 nm in thickness was deposited on the soda-lime glass by DC magnetron sputtering. All the substrates were cleaned and finally dried by blowing N_2 gas. The Zn/(Cu,Sn) metal precursor was deposited by RF magnetron sputtering using quaternary target consisting of Cu (99.995%), Zn(99.999%) and Sn(99.999%) with 7.5 cm in diameter and stoichiometric (Cu: 25%, Zn: 12.5%, Sn; 12.5% and S: 50%). After the base pressure reached approximately 4×10^{-5} Torr, precursor was deposited at a working pressure of 0.67 Pa in an Ar atmosphere. RF power and Time were 40 Watt and 160 min. respectively.

The grown films were annealed in three capsules with different annealing temperatures at 200 ^{0}C, 350 ^{0}C and 500 ^{0}C for 60 min in vacuum. The CZTS thin films annealed at higher than 550°C and longer that 60 min. were decomposed, which limits the annealing temperature below than 550°C for 60 min. Before and after each annealing stage, the structural and optical properties were measured. The crystal structure and phase composition of the CZTS thin films were established by X-ray diffraction (XRD) analysis in the range of scattering angles $2\theta = 10^0 - 80^0$. The XRD patterns were recorded by an automatically controlled Siemens D-5000 diffract meter operating at CuK_α radiation (λ = 1.5405 Å) and a nickel filter. The transmittance and reflectance spectra of the experimental samples were recorded in the wavelength range 300–900 nm using a Cary-500 Scan (Varian, USA) spectrophotometer with a spectral resolution of 1.0 nm. These data were used to analyze the optical properties and the parameters for the optical absorption edge of the films.

3. RESULTS AND DISCUSSION

Figure 1 shows the XRD patterns of CZTS thin films deposited by RF magnetron sputtering on the glass substrate and annealed at different temperatures. The identification and assignments of the observed diffraction patterns were made using the JCPDS data and reported literature [11]. The intensity of the (112)

CZTS and (211) Mo reflection of picks increases with the annealing temperature. This pattern showed
several peaks produced by the (112) and (312) crystalline planes of the tetragonal CZTS phase It shows that CZTS thin films annealed at the higher has the better crystalline property. The average grain size can be calculated from the Scherrer equation [12]. The peaks of the preferred orientation (112) show higher intensities and larger grain size. The X-ray diffraction peaks obtained at (312) correspond to Kesterite CZTS with tetragonal phase [13, 14].

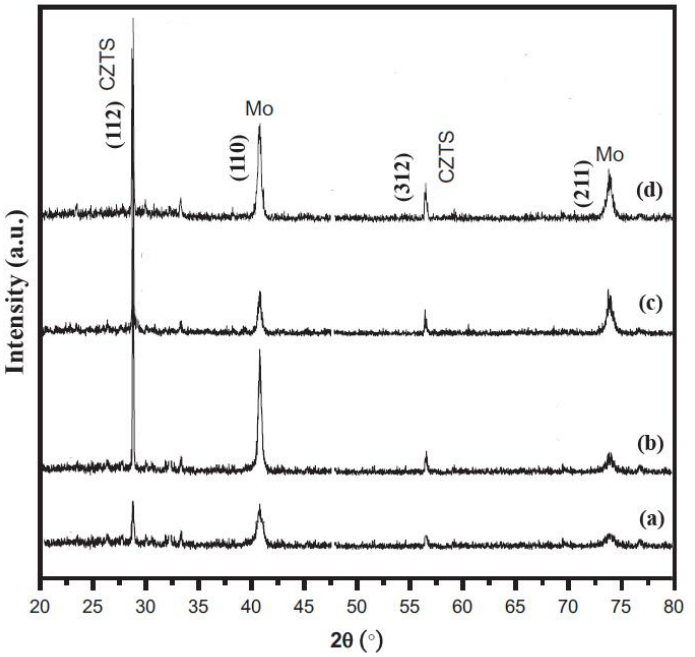

Fig. 1. X-ray diffraction spectra of the CZTS thin films annealed at various temperatures for 60 min. (a)- before annealing, (b) annealed at 200 ^{0}C, (c) annealed at 350 ^{0}C (d) annealed at 500 ^{0}C.

Lattice parameters from the XRD pattern were determined from the formula [15]:

$$a_{i,j}^2 = \frac{\lambda^2}{4} \cdot \frac{A_i B_j - A_j B_i}{B_j \mathrm{Sin}^2\theta_i - B_i \mathrm{Sin}^2\theta_j} \quad (1)$$

$$c_{i,j}^2 = \frac{\lambda^2}{4} \cdot \frac{A_i B_j - A_j B_i}{A_i \mathrm{Sin}^2\theta_j - A_j \mathrm{Sin}^2\theta_i} \quad (2)$$

Where θ is the scattering angle and $A = h^2 + k^2$, $B = l^2$ the parameters calculated and listed in Table 1. Morphology and surface topology of the as deposited and

annealed films were studied by AFM. The AFM images are shown in Figure 2. This images show clear grain boundary between smaller grains before annealing and growth of grain size by increasing the annealing temperature.

Table 1: Calculated lattice parameters from the XRD spectra of CZTS thin films

Sample	2ɵ	peak	a(^{0}A)	c(^{0}A)
Annealed at 200 ^{0}C	28.6	(112)	5.41	10.80
annealed at 350 ^{0}C	28.6	(112)	5.41	10.80
annealed at 500 ^{0}C	28.6	(112)	5.41	10.80
annealed at 500 ^{0}C	56.1	(312)	5.43	10.89

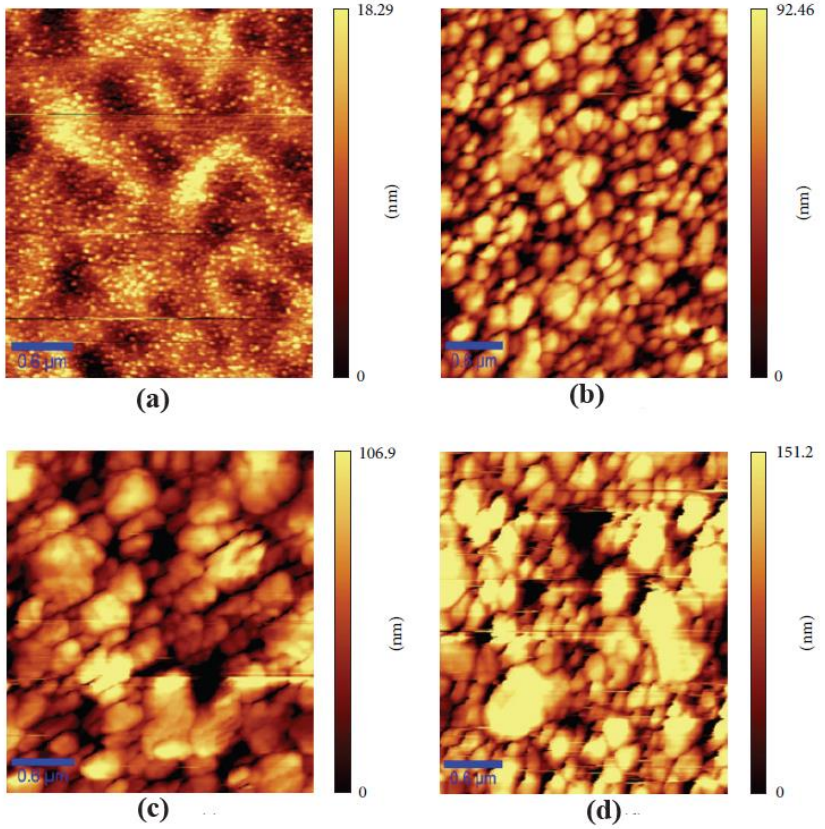

Fig. 2. AFM images of CZTS thin films, (a) before annealing, (b) annealed at 200 ^{0}C, (c) annealed at 350 ^{0}C (d) annealed at 500 ^{0}C.

Figure 3 shows the surface and cross-sectional SEM images of the as-deposited and the annealed CZTS samples prepared RF magnetron sputtering method. The crystallinity changes could be perceptibly found. After annealing the texture of the CZTS thin film transformed from thin grains to equiaxial grain structure. After annealing particles adopted sharper edges and increased grain size than as deposited films and shows that thickness of CZTS thin films increase as annealing temperature increased. Slight decrease in the roughness and micro cracks were observed with increasing the annealing temperature which is consistent with the reported literature [16] .Therefore the particle size and thickness of CZTS become larger with increasing annealing temperature. The roughness values of the CZTS thin films are given in Table 2. The roughness values increased remarkably after annealing because annealing acts as thermal etching of the film surface [17]. During annealing agglomerated particles are formed due to coalescence of small grain together, this also led to increased roughness value (Figure 4).

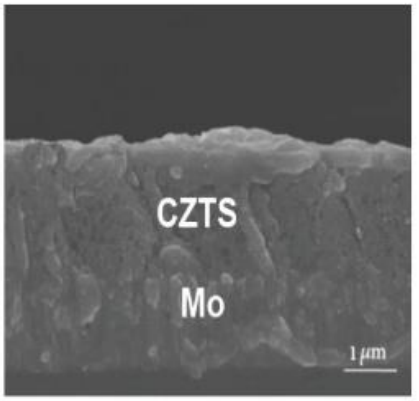

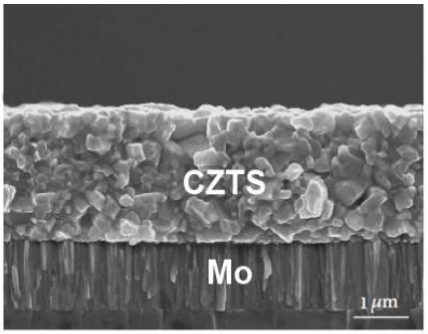

Fig. 3. Typical SEM images of CZTS thin films, (a) before annealing, (b) annealed at 200 ^{0}C, (c) annealed at 500 ^{0}C

The Raman spectrum shown in Fig. 5 for the CZTS sample before and after annealing. It shows the presence of two major peaks at 282 and 332 cm^{-1} which can be attributed to tetragonal and cubic CZTS respectively [18]. The presence of the shoulder peaks at 370 cm^{-1} confirm the formation of kesterite CZTS. No other peaks are observed for the CZTS thin films before and after annealing [19, 20].

Table 2 Roughness of CZTS thin films deposited at different temperatures before and after annealing [2 base main paper]

Sample	**Roughness (nm)**
Before annealing,	8.9
Annealed at 200 ^{0}C	11.2
Annealed at 350 ^{0}C	18.5
Annealed at 500 ^{0}C	27.4

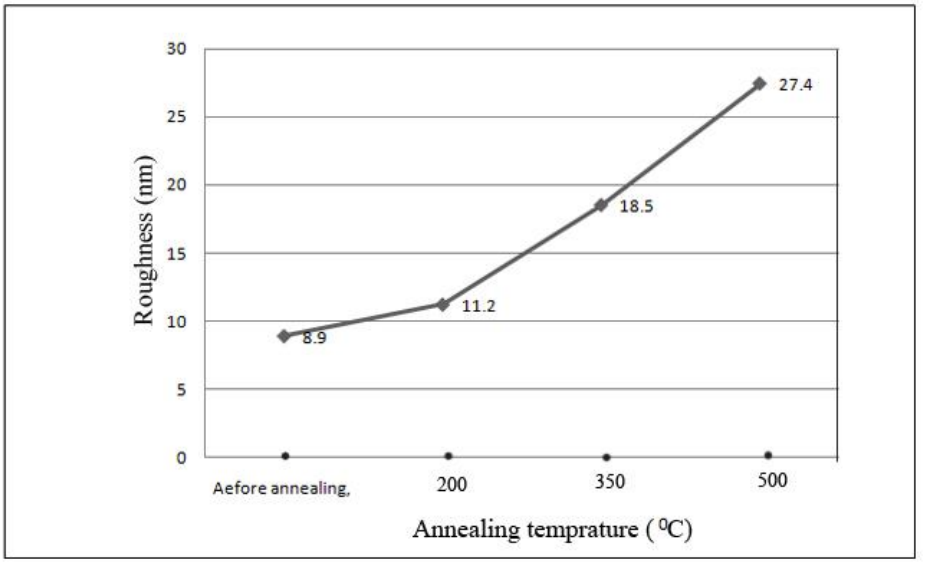

Fig. 4. Surface roughness of as-sputtered and annealed films analyzed by AFM measurement.

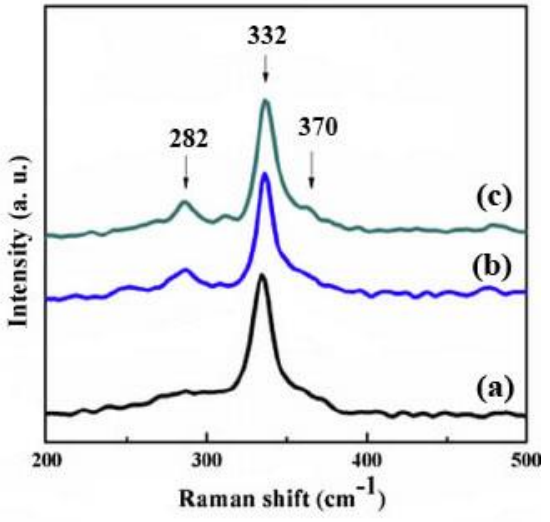

Fig. 5. Raman patterns of CZTS thin films, (a) before annealing, (b) annealed at 350 ^{0}C and (c) annealed at 350 ^{0}C.

The optical transmittance spectra of (a) as deposited and (b) annealed CZTS thin films, in the wavelength range of 300–900 nm, are shown in Figure 6(I) and the

Tauc curves calculated from the transmittance curves are shown in Figures 6(II) [21].

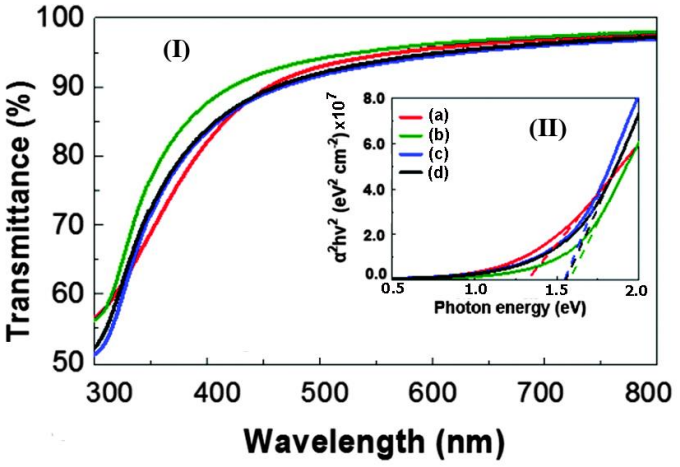

Fig. 6. Transmittance (I) and absorption coefficient (II) spectra of CZTS thin films, (a) annealed at 500 ^{0}C before annealing, (b) annealed at 200 ^{0}C, (c) annealed at 350 ^{0}C (d) before annealing

The energy band gap (E_g) of the CZTS thin films was calculated before and after annealing from the transmittance spectra using Beer-Lambert's law. Results show that E_g is dependent on the annealing temperature. The annealed CZTS thin films at 500 ^{0}C have lower optic energy band gap compared with the as-deposited samples. The optical band gap of CZT varied from 1.59 eV (before annealing) to 1.31 (500 ^{0}C) eV with increase in the annealing temperature. These results indicate that the annealed films present higher crystallinity that is consistent with the XRD measurements [22, 23].

4. CONCLUSION

In this paper we have investigated the effect of annealing on the phase formation, crystallite size, optical band gap and Raman spectroscopy of Mo/CZTS thin films fabricated by RF magnetron sputtering. The intensity of (112) peak of CZTS layer in XRD patterns and the grain size increased after annealing. The shape of crystallite also improved with annealing temperature. The optical band gap of CZTS also varied from 1.57 eV to 1.31 eV with increase in the annealing temperature from 200 ^{0}C min to 500 ^{0}C, respectively. Shifts in the Raman spectra have been observed with increase in the annealing temperature. Both the increase

of the optical transmittance and the grain structure after annealing lead to the improved performance of thin-film CZTS solar cells.

5. ACKNOWLEDGEMENT

The authors would like to thank Marvdasht Branch, Islamic Azad University for the financial support of this research, which is based on a research project contract**.**

REFERENCES

[1] K. Ito and T. Nakazawa. *Electrical and optical properties of stannite-type quaternary semiconductor thin films*. Jap J. App. Phys. 27 (1988) 2094– 2097.

[2] H. Katagiri. N. Sasaguchi. S. Hando. S. Hoshino. J. Ohashi, and T. Yokota. *Preparation and evaluation of Cu2ZnSnS4 thin films by sulfurization of e-b evaporated precursors*. Sol Energy Mater Sol. Cells. 49 (1997) 407–414.

[3] K. Diwatea. K. Mohiteb. M. Shindec. S. Rondiyaa. A. Pawbakea. *Synthesis and characterization of chemical spray pyrolysed CZTS thin films for solar cell applications.* Energy Procedia. 110 (2017) 180 – 187.

[4] N. Thota.·M. Gurubhaskar. A. C. Kasi. G. Hema Chandra. B. R. Mehta. A. Tiwari. Y. P. Venkata Subbaiah. *Growth and properties of Cu2ZnSnS4 thin films prepared by multiple metallic layer stacks as a function of sulfurization time*. J Mate Sci Mater Electron. 28 (2017) 11702–11711.

[5] N. Nakayama, and K. Ito. *Sprayed films of stannite Cu2ZnSnS4*. App. Surf. Sci. 92 (1996) 171–175.

[6] W. Shockley. and H. J. Queisser. *Detailed Balance Limit of Efficiency of p-n Junction Solar Cells*. J. App. Phys. 32 (1961) 510–519.

[7] R. Chalapathy. G. Jung. B. Ahn. *Fabrication of Cu2ZnSnS4 films by sulfurization of Cu/ZnSn/Cu precursor layers in sulfur atmosphere for solar cells Sol.* Energy Mater Sol. Cells. 95 (2011) 3216–3221.

[8] A. Chirila. P. Reinhard. F. Pianezzi. P. Bloesch. A. R. Uhl. C. Fella. *Potassium-induced surface modification of Cu(In,Ga)Se2 thin films for high-efficiency solar cells*. Nat. Mater. 12 (2013) 1107–1111.

[9] A. Emrani. P. Vasekar. C. R. Westgate. *Effects of sulfurization temperature on CZTS thin film solar cell performances*. Sol. Energy. 98 (2013) 2855–2860.

[10] A. Fairbrother. X. Fontane. V. Izquierdo-Roca. M. Espíndola-Rodríguez. S. López-Marino and M. Placidi. *On the formation mechanisms of Zn-rich Cu2ZnSnS4 films prepared by sulfurization of metallic stacks.* Sol. Energy Mater Sol. Cells. 112 (2013) 97–105.

[11] J. Lee. H. Choi. W. Kim. *Effect of pre-annealing on the phase formation and efficiency of CZTS solar cell prepared by sulfurization of Zn/(Cu,Sn) precursor with H2S gas.* Sol. Energy. 136 (2016) 499–504.

[12] J. Leitao. N. M. Santos. P.A. Fernandes. *Study of optical and structural properties of Cu 2 ZnSnS 4 thin films*. Thin Solid Films. 519 (2011) 7390–7393.

[13] JCPDS 26-0575.

[14] A. Patterson. *The Scherrer Formula for X-Ray Particle Size Determination*. Phys Rev. 56 (1939) 978–982.

[15] Bragg, W.L. The Crystalline State: Volume I. New York, Macmillan Company, 1934, 123–135.

[16] M. Altosaar. J. Raudoja. K. Timmo. M. Danilson. M. Grossberg. J. Krustok. and E. Mellikov. *Sulfur-containing Cu2ZnSnSe4 monograin powders for solar cells.* Phys Stat Sol 205(a) (2008) 167–170.

[17] M. Xie. D. Zhuang. M. Zhao. B. Li. M. Cao. and J. Song. *Fabrication of Cu2ZnSnS4 thin films using a ceramic quaternary target*. Vacuum. 101 (2014) 146–150.

[18] H. Katagiri. K. Jimbo. S. Yamada. T. Kamimura. W. S. Maw. T. Fukano. *Enhanced conversion efficiencies of. Cu2ZnSnS4-based thin film solar cells by using preferential etching technique*. Appl Phys Exp. 1 (2008) 041201-041202.

[19] M.P. Suryawanshi. S. W. Shin. U. V. Ghorpade. K. V. Gurav. C. W. Hong. P. S. Patil. A. V. Moholkar and J. H. Kim. *Improved solar cell performance of Cu2ZnSnS4 (CZTS) thin films prepared by sulfurizing stacked precursor thin films via SILAR method*. J Alloys Compd. 671 (2016) 509-516.

[20] H. Park. Y. H. Hwang. and B. Bae. *Sol-gel processed Cu2ZnSnS4 thin films for a photovoltaic absorber layer without sulfurization*. J Sol-Gel Sci. Technol. 65 (2013) 23–27.

[21] W. Liu. B. Guo. C. Mak. A. Li. X. Wu. and F. Zhang. *Facile synthesis of ultrafine Cu2ZnSnS4 nanocrystals by hydrothermal method for use in solar cells*. Thin Solid Films. 535 (2013) 39–43.

[22] H. Miyazaki. M. Aono. H. Kishimura. K. Jimbo. H. Katagiri. *Annealing behaviour of photoluminescence spectra on Cu2ZnSnS4 single crystals.* Phys Status Solidi C. 14 (2017) 1-4.

[23] M.A. Olgar. J. Klaer. L. Ozyuzer, T. Unold. *Cu2ZnSnS4-based thin films and solar cells by rapid thermal annealing processing*. Thin Solid Films. 628 (2017) 1–6.